

# Fictitious fluxes in doped antiferromagnets

Stellan Östlund and Martin Andersson  
*Department of Theoretical Physics and Mechanics,  
 Chalmers University of Technology and Göteborg University,  
 S-412 96 Göteborg, Sweden*  
 (November 20, 2018)

In a tight binding model of charged spin- $\frac{1}{2}$  electrons on a square lattice, a fully polarized ferromagnetic spin configuration generates an apparent  $U(1)$  flux given by  $2\pi$  times the skyrmion charge density of the ferromagnetic order parameter. We show here that for an antiferromagnet, there are two “fictitious” magnetic fields, one staggered and one unstaggered. The staggered topological flux per unit cell can be varied between  $-\pi \leq \Phi \leq \pi$  with a negligible change in the value of the effective nearest neighbor coupling constant whereas the magnitude of the unstaggered flux is strongly coupled to the magnitude of the second neighbor effective coupling.

## GENERAL PROPERTIES OF SPIN GENERATED FLUXES

It is well known that in the theory of the quantum Hall problem spin textures can generate an effective  $U(1)$  flux which acts as an effective magnetic field leading to an association between topological and electrical charge.<sup>1</sup> In this paper we investigate to what extent this effect can be generalized to the antiferromagnet.

For definiteness, we consider the  $t$ - $J$  model on a square lattice. This model is described by the Hamiltonian

$$H = \sum_{\langle ij \rangle} \left[ -(t^{ij} c_{i\sigma}^\dagger c_{j\sigma} + \text{h.c.}) + J^{ij} (\mathbf{S}_i \cdot \mathbf{S}_j - \frac{1}{4} n_i n_j) \right] \quad (1)$$

where the summation runs over nearest neighbor pairs  $\langle ij \rangle$  and  $\mathbf{S}_i = c_{i\alpha}^\dagger \vec{\sigma}_{\alpha\beta} c_{i\beta}$  and  $\vec{\sigma}$  denotes the vector of Pauli matrices. All states containing doubly occupied sites have been excluded from the Hilbert space. [For a general reference, see Ref. 2.]

To make explicit the connection between spin rotations and effective couplings, we introduce a local change of spin coordinates [see for instance Ref. 3], choosing the local spin quantization axis at site  $i$  along  $\hat{\Omega}_i$ . The action of this local  $SU(2)$  transformation on  $c_i$  is written

$$c_i \longrightarrow U_{\hat{\Omega}_i} c_i, \quad (2)$$

where

$$U_{\hat{\Omega}_i} \sigma_z U_{\hat{\Omega}_i}^\dagger = \hat{\Omega}_i \cdot \vec{\sigma}. \quad (3)$$

The specification of  $\hat{\Omega}_i$  fixes  $U_{\hat{\Omega}_i}$  only up to an overall rotation about the new local  $z$ -axis. Choosing  $G_i = \exp[-i\frac{1}{2}\alpha_i \hat{\Omega}_i \cdot \vec{\sigma}]$  makes  $U_{\hat{\Omega}_i}' = G_i U_{\hat{\Omega}_i}$  also satisfy the defining relation, Eq. (3). To fix this remaining degree of freedom, we arbitrarily choose  $U_{\hat{\Omega}_i}$  to correspond to a

rotation about an axis lying in the spin  $x$ - $y$  plane. Defining the unit vector  $\hat{\omega}_i = (\hat{z} \times \hat{\Omega}_i) = (-\sin \phi_i, \cos \phi_i, 0)$  we have

$$U_{\hat{\Omega}_i} = \exp[i\frac{1}{2}\theta_i \hat{\omega}_i \cdot \vec{\sigma}] = \cos(\frac{1}{2}\theta_i) + i \sin(\frac{1}{2}\theta_i) \hat{\omega}_i \cdot \vec{\sigma}, \quad (4)$$

where  $\cos \theta_i = \hat{z} \cdot \hat{\Omega}_i$ .

We then find the following Hamiltonian in the new spin coordinate system

$$H = \sum_{\langle ij \rangle} \left[ -(t^{ij} c_{i\alpha}^\dagger M_{\alpha\beta}^{ij} c_{j\beta} + \text{h.c.}) + J^{ij} (S_i^\alpha S_j^\beta Q_{\alpha\beta}^{ij} - \frac{1}{4} n_i n_j) \right], \quad (5)$$

where we have introduced  $M^{ij} = (U_{\hat{\Omega}_i})^\dagger U_{\hat{\Omega}_j}$ ,  $Q^{ij} = R_{\hat{\Omega}_i}^{-1} R_{\hat{\Omega}_j}$ , and  $(R_{\hat{\Omega}})_{ij} = \cos \theta \delta_{ij} + (1 - \cos \theta) \omega_i \omega_j + \sum_k \sin \theta \epsilon_{ijk} \omega^k$  is the  $SO(3)$ -rotation operator induced by  $U_{\hat{\Omega}}$ .

Until this point, the discussion has been completely general. In order to make further progress, we neglect spin fluctuations and make the restriction that a site is occupied by at most one spin and that the electron which occupies site  $i$  has its spin pointing along the local positive  $z$ -axis,  $\hat{\Omega}_i$ . This constraint reduces Eq. (5) to

$$H_{\text{eff}} = \sum_{\langle ij \rangle} \left[ -(\tau^{ij} c_i^\dagger c_j + \text{h.c.}) + K^{ij} n_i n_j \right], \quad (6)$$

with  $\tau^{ij} = t^{ij} M_{11}^{ij}$ ,  $K^{ij} = \frac{1}{4} J^{ij} (\hat{\Omega}_i \cdot \hat{\Omega}_j - 1)$ , and  $c_j \equiv c_{j1}$ . At this point we have an effective model describing “spinless” fermions on a lattice with hopping amplitudes and interaction-strengths being functions of position. In this way we have automatically solved the constraint of no double occupancies at the expense of treating the spins as classical variables and ignoring their quantum spin fluctuations.

Let us now turn to the properties of  $\tau^{ij}$ . First we note that  $\tau^{ij} = (\tau^{ji})^*$ . The complex phase of  $\tau^{ij}$  cannot in general be gauged away by a local transformation  $c_j \rightarrow e^{i\phi_j} c_j$  if the spin configurations are noncoplanar. When we defined the local transformation  $U_{\widehat{\Omega}_i}$ , we noted that it was only specified up to a rotation about the local  $z$ -axis,  $U_{\widehat{\Omega}} \rightarrow GU_{\widehat{\Omega}}$ . The effect of such a local rotation on the effective hopping cannot be distinguished from a local gauge transformation  $c_i \rightarrow e^{i\frac{1}{2}\alpha_i} c_i$  which does not affect the physics. Hence, the set of physically inequivalent choices of  $U_{\widehat{\Omega}_i}$  belong to  $SU(2)/U(1) \cong S^2$  and we conclude that in the absence of an external magnetic field, there are two physical degrees of freedom per site (or plaquette) which determine the effective coupling constants.

To understand more precisely which portions of the effective hopping  $\tau^{ij}$  are  $U(1)$  gauge invariant, we look at a particular plaquette of the lattice, consisting of points labelled counterclockwise as  $r_0, r_1, r_2$ , and  $r_3$  and with associated spins pointing in the  $\Omega_i$  directions. The flux through the plaquette is given by

$$\Phi_{\text{plaquette}} = \text{Im} \ln (\tau^{r_0 r_1} \tau^{r_1 r_2} \tau^{r_2 r_3} \tau^{r_3 r_0}). \quad (7)$$

Topological arguments show that  $\Phi_{\text{plaquette}} = \frac{1}{2}\mathcal{A}(\widehat{\Omega}_0, \widehat{\Omega}_1, \widehat{\Omega}_2, \widehat{\Omega}_3)$ , half the solid angle enclosed by the shortest path on the sphere connecting the vectors  $\{\widehat{\Omega}_i\}$ , i.e. the flux corresponding to the plaquette is equal to  $2\pi$  times the skyrmion charge represented by the plaquette. Generalizing a result of Wen, Wilczek, and Zee<sup>4</sup> who computed the imaginary part of the formula below one may show that for a plaquette consisting of exactly three sites

$$\tau^{r_0 r_1} \tau^{r_1 r_2} \tau^{r_2 r_0} = \frac{1}{8} \left[ (\widehat{\Omega}_0 + \widehat{\Omega}_1 + \widehat{\Omega}_2)^2 - 1 \right] + \frac{i}{4} \widehat{\Omega}_0 \cdot (\widehat{\Omega}_1 \times \widehat{\Omega}_2). \quad (8)$$

Assuming smooth fields  $\theta(\mathbf{r})$  and  $\phi(\mathbf{r})$  one finds in the continuum limit that the fictitious flux corresponds to a Berry gauge field

$$\mathcal{A}_\mu = \langle \widehat{\Omega} | \partial_\mu | \widehat{\Omega} \rangle = i \sin^2 \frac{\theta}{2} \partial_\mu \phi,$$

which is the vector potential due to a magnetic monopole of strength  $-\frac{1}{2}$ . The local  $U(1)$  degree of freedom, represented by the  $G$ 's, corresponds to a gauge transformation of the topological vector potential  $\mathcal{A}_\mu$ .

### The case of the ferromagnet

Let us now consider the plaquette  $(\widehat{\Omega}_0, \widehat{\Omega}_1, \widehat{\Omega}_2, \widehat{\Omega}_3)$  in spin space, drawn as in Fig. 1, the parallelogram representing a patch of the surface of the sphere. To simplify the argument further, we restrict ourselves to the case  $\widehat{\Omega}_i \cdot \widehat{\Omega}_j = \cos \theta$  for all nearest neighbor pairs  $\langle ij \rangle$  in the

plaquette, so that the relative angle between the spins on each side of the square is  $\theta$ . A straightforward application of spherical geometry yields the relation  $\frac{1}{2}\mathcal{A} = (\alpha + \beta) - \pi$  where  $\alpha$  and  $\beta$  are the interior surface angles of the spherical parallelogram.

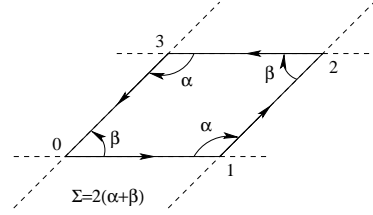


FIG. 1. The close to ferromagnetic spin-configuration is shown in spin-space. All sides in this spherical parallelogram correspond to an opening angle  $\theta$ .  $\Sigma$  denotes the sum of the angles within the path  $0 \rightarrow 1 \rightarrow 2 \rightarrow 3 \rightarrow 0$ .

However, since  $\theta$  is fixed on all sides, we cannot freely choose  $\alpha$  and  $\beta$ . Rather, we solve for  $\Phi = \frac{1}{2}\mathcal{A}$  in terms of  $\alpha - \beta$  and  $\theta$  and then derive expressions for the nearest-neighbor coupling constants  $\tau$  and  $K$  in terms of the same variables. Using standard formulas from spherical geometry together with Eq. (4) we find

$$\begin{aligned} |\tau_{nn}| &= \cos(\frac{1}{2}\theta) \\ \Phi &= 2 \arcsin(\tan^2(\frac{1}{2}\theta) \cos(\frac{1}{2}(\alpha - \beta))) \\ K &= \frac{1}{4}J(\cos \theta - 1), \end{aligned} \quad (9)$$

where  $\tau_{nn}$  is the effective nearest-neighbor hopping amplitude. We note that  $\Phi$  is given by  $\Phi = \frac{1}{2}\theta^2 \cos(\frac{1}{2}(\alpha - \beta))$  for small  $\theta$ .

### The case of antiferromagnetic order

Let us now consider the analogous calculations for a spin configuration which is close to antiferromagnetic. Let us denote the local antiferromagnetic spin as  $\widehat{\Omega}_i$  as before. Denote by  $\widehat{\Omega}'_i = -\widehat{\Omega}_i$  the antipodal points. Noting that in the case of a spherical parallelogram, great circles which connect the four sides of  $\{\widehat{\Omega}_i\}$  intersect in the points  $\{\widehat{\Omega}'_i\}$ , we find that the path  $\widehat{\Omega}_0 \rightarrow \widehat{\Omega}'_1 \rightarrow \widehat{\Omega}_2 \rightarrow \widehat{\Omega}'_3 \rightarrow \widehat{\Omega}_0$  connecting the antiferromagnetic spins has the geometry sketched in Fig. 2. Fig. 3 shows another illustration of the path taken in spin space when going around a plaquette in an antiferromagnetic background. By using Eq. (4) the angles  $\alpha$  have become exterior rather than interior angles in the path. This gives us the relations

$$\begin{aligned} |\tau_{nn}| &= \sin(\frac{1}{2}\theta) \\ \Phi &= \pi - (\alpha - \beta) \\ K &= -\frac{1}{4}J(\cos \theta + 1) \end{aligned} \quad (10)$$

where in this case  $\cos \theta = -\widehat{\Omega}_i \cdot \widehat{\Omega}'_{i+1}$ . Comparing to Eq. (9) we see that the connection between  $\theta$  and  $\Phi$  has disappeared.

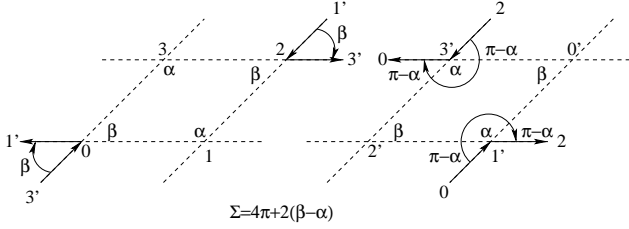


FIG. 2. The close to antiferromagnetic spin-configuration is shown in spin-space. The left part corresponds to the points  $\widehat{\Omega}_i$ , while the right part corresponds to the antipodal points  $\widehat{\Omega}'_i$ . It is seen how the  $\alpha$ -angles become exterior rather than interior leading to a completely different  $\Sigma$  as compared to the ferromagnetic case.

By extending the same argument to the adjacent cell, we reproduce the arguments, however all paths are traversed in the opposite sense and the flux becomes negative compared to the first cell. The flux is therefore staggered, with a  $\pm$  sign depending on the sign of the sublattice associated with the plaquette.

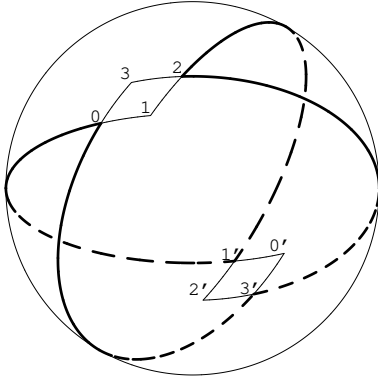


FIG. 3. The path taken in spin-space when going around a plaquette  $0 \rightarrow 1' \rightarrow 2 \rightarrow 3' \rightarrow 0$  in an antiferromagnetic background. All paths follow great circles on the sphere.

In contrast to the case of the ferromagnet, we find that we can change the effective staggered flux for the electron gas, Eq. (6), from  $-\pi$  to  $\pi$  without affecting the magnitude of the local values of the effective nearest neighbor coupling constants. In fact, for the most symmetric case  $\alpha = \beta$ , we find that an antiferromagnetic skyrmion generates an effective staggered flux of exactly  $\pi$  per plaquette. Due to the curvature of the sphere, such a texture cannot in general be extended to the plane.

## Next-nearest neighbor hopping

When we include second neighbor hopping, the situation becomes much more complicated for the antiferromagnet. Each square plaquette has four gauge invariant fluxes, corresponding to each triangle defined by the removal of one vertex from the four corners of the square. When the spins are aligned close to ferromagnetically, the shortest path in spin space connecting the two diagonal spins lies wholly within the region defined by the corner spins. Hence the flux through each triangular subplaquette is very closely proportional to the area of each subtriangle in real space, and the sum of flux through a pair of subtriangles that cover the square is precisely equal to the flux through the entire plaquette. As a consequence, the effective phase of each of the interactions is extremely well approximated by spreading a constant effective magnetic field corresponding to the local skyrmion density throughout the entire real space plaquette and assigning the effective phase on the links by a conventional choice of gauge<sup>5</sup>.

In the case of a configuration close to antiferromagnetic, the four subtriangles cover the entire sphere in spin space [see Fig. 3]. Taking into account the orientation of each of the bounding paths, we find the following relation between the flux through each of the triangles for both the ferromagnet and antiferromagnet:

$$\begin{aligned} \Phi(\widehat{\Omega}_0\widehat{\Omega}_1'\widehat{\Omega}_2) + \Phi(\widehat{\Omega}_0\widehat{\Omega}_2\widehat{\Omega}_3') \\ - \Phi(\widehat{\Omega}_0\widehat{\Omega}_1'\widehat{\Omega}_3') - \Phi(\widehat{\Omega}_1'\widehat{\Omega}_2\widehat{\Omega}_3') = 2\pi n, \end{aligned} \quad (11)$$

where  $n = 0$  for the ferromagnet and  $n = \pm 1$  for the antiferromagnet. Note that Eq. (11) is valid in general, i.e. it does not rely on the assumption of a spherical parallelogram. It is also easy to see that it is valid in the presence of an external electromagnetic flux. If we assume a spherical parallelogram we can also note from Fig. 2 that  $\Phi(\widehat{\Omega}_0\widehat{\Omega}_1'\widehat{\Omega}_3') = \Phi(\widehat{\Omega}_1'\widehat{\Omega}_2\widehat{\Omega}_3') = \frac{1}{2}\Phi$ . It therefore follows that  $\Phi(\widehat{\Omega}_1'\widehat{\Omega}_2\widehat{\Omega}_0) = \Phi(\widehat{\Omega}_0\widehat{\Omega}_2\widehat{\Omega}_3') = \frac{1}{2}\Phi + n\pi$ . Hence, for the antiferromagnet, links connecting sites within the same sublattice pick up a phase  $\pi$  if they belong to sublattice  $A$ , and zero if they belong to sublattice  $B$ , or vice versa.<sup>6</sup>

In Fig. 4 is drawn a  $3 \times 3$  subset of a 2D antiferromagnetic lattice. The value of the local spin generated phase  $\text{Im} \ln(M_{11}^{ij}) \equiv \phi_{ij}$  is indicated on each link. Arrows indicate the direction  $i \rightarrow j$ . The gauge is chosen so that  $\phi_{r,r+\hat{x}} = 0$ . The phase  $\phi_{r,r+\hat{y}} = \frac{(-1)^r}{2}\Phi$ . Along the diagonals, the phase of the coupling constant is:

$$\begin{aligned} \phi_{r,r+\hat{y}+\hat{x}} &= \frac{\pi}{2}[1 + (-1)^r] \\ \phi_{r+\hat{x},r+\hat{y}} &= \frac{\pi}{2}[1 - (-1)^r]. \end{aligned} \quad (12)$$

The local gauge choice does not take account of the curvature of the spin space and in general, the sphere cannot be covered with parallelograms so the local choice

of gauge cannot be extended to the whole sphere. Nevertheless, in the limit  $\theta \rightarrow 0$  the above formula is expected to be valid.

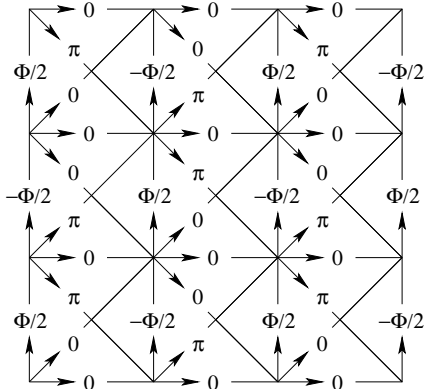


FIG. 4. A particular choice of gauge for the staggered flux-phase ( $\pm\Phi$ ) with next-nearest neighbor hopping is indicated through the phases associated with each link in the lattice.

An intriguing special choice for  $\theta$  where it is possible to cover the sphere by parallelograms is  $\cos\theta = -1/3$ . In this case, the spins reside on the vertices of a regular tetrahedron, and it is also possible to extend this mapping exactly over a square lattice. Considering that going around a plaquette in the real space lattice, corresponds to encircling two of the faces of the tetrahedron, it is obvious that this loop will cover half of the spin-sphere and hence the “tetrahedral phase” generates a staggered flux  $\pm\pi$ .

Putting all this together, we find that given original nearest ( $t_{nn}$ ) and next nearest neighbor hopping ( $t_{nnn}$ ), the effective coupling constants for the remaining fermionic degrees of freedom are determined by the two free parameters  $\theta$  and  $\Phi$  which control the unstaggered and staggered fluxes, respectively. In the general case with an external electromagnetic flux we have  $2 + 1$  physical degrees of freedom per plaquette. This results in three independent fluxes per square, the only restriction being given by Eq. (11). Using standard formulas from spherical geometry, we find that with a suitable choice of gauge, the effective nearest and next nearest neighbor couplings are given by:

$$\begin{aligned}
 \tau_{nn} &= t_{nn} \sin(\frac{1}{2}\theta) \\
 \tau_{r+\hat{x}} &= \tau_{nn} \\
 \tau_{r+\hat{y}} &= \tau_{nn} e^{i(-1)^r \Phi/2} \\
 \cos(\theta_+ \pm \theta_-) &= \cos(\theta) \pm (1 - \cos(\theta)) \sin(\frac{1}{2}\Phi) \\
 \tau_{r,r+\hat{x}+\hat{y}} &= (-1)^{r+1} t_{nnn} \cos(\theta_+) \\
 \tau_{r+\hat{y},r+\hat{x}} &= (-1)^r t_{nnn} \cos(\theta_-).
 \end{aligned} \tag{13}$$

## CONCLUSION

The main conclusion from this paper is that in contrast to the ferromagnet, antiferromagnetic spin textures naturally generate a staggered flux<sup>7</sup> on the basic nearest neighbor plaquettes. However, in contrast to case of the ferromagnet, the amount of flux per plaquette is weakly related to the *magnitude* of the effective nearest neighbor coupling. Incorporating second neighbor interactions reveals the existence of an additional independent effective  $U(1)$  fictitious flux on plaquettes of second neighbor sites. Since the first neighbor coupling is severely suppressed in a Néel antiferromagnet, it is quite possible that the effective second neighbor interactions could be important; in the limit of weakly coupled effective nearest neighbors and strongly coupled second neighbors textures such as appear in the two layer quantum Hall problem could be favored.<sup>8</sup> However, even in this case the magnetic field energy generated by staggered orbital currents could suppress these textures.<sup>9</sup>

Using Eq. (13) we<sup>10</sup> have numerically calculated energies of various uniform spin textures in the Hartree-Fock approximation and for nonuniform stripe textures in the Hartree approximation, with the goal of understanding if noncoplanar spin textures which generate fictitious staggered flux have lower energy than the coplanar “spiral” phases studied previously by a number of authors.<sup>3,11,12</sup> Preliminary results are consistent with those that have been obtained previously by more elaborate means; spiral phases appear to have the lowest energy for the uniform phases but are thermodynamically unstable against phase separation. The noncoplanar phases all have staggered fictitious rather than the unstaggered flux which is known to lower the kinetic energy in an electron gas and there does not appear to be any clear association between topological charge and doping, at least in a tight binding model dominated by nearest neighbor interactions.<sup>13</sup>

By neglecting quantum spin fluctuations as we have done, our numerical simulations of the nonuniform spin textures suffer from the same problem as others who similarly ignore spin fluctuations. The ordinary Néel antiferromagnet becomes insulating, and this, together with the tendency towards phase separation apparently does not favor noncoplanar spin textures with any nontrivial topological properties. It remains to be seen if properly accounting for quantum spin fluctuations can change this result.

<sup>1</sup> S. C. Zhang, T. H. Hansson, and S. A. Kivelson, Phys. Rev. Lett. **62**, 82 (1989); A. Karlhede, S. A. Kivelson, K. Lejnell, and S. L. Sondhi, Phys. Rev. Lett. **77**, 2061 (1996); D. H. Lee and C. L. Kane, Phys. Rev. Lett. **64**, 1313 (1990).

<sup>2</sup> See for instance E. Fradkin, *Field Theories of Condensed*

*Matter Physics*, Addison Wesley (1991) and references therein.

<sup>3</sup> H. J. Schulz, Phys. Rev. Lett. **65**, 2462 (1990).

<sup>4</sup> The imaginary part of this expression was pointed out by X. G. Wen, F. Wilczek, and A. Zee, Phys. Rev. B. **39**, 11413 (1989).

<sup>5</sup> W. Barford and J. H. Kim, Phys. Rev. B **43**, 559 (1991).

<sup>6</sup> By multiplying  $c_r^\dagger$  by  $(-1)$  if  $r \cdot \hat{x}$  and  $r \cdot \hat{y}$  are odd, we can gauge away the staggered minus sign in the diagonal phases at the price of introducing an additional staggered component in the nearest neighbor couplings.

<sup>7</sup> I. Affleck and J. B. Marston, Phys. Rev. B **37**, R3774 (1987).

<sup>8</sup> S. M. Girvin, *The Quantum Hall Effect, Novel Excitations and Broken Symmetries*, Les Houches Lectures, 1998. Published by Springer Verlag (1999). See also cond-mat/9907002.

<sup>9</sup> A. B. Harris, T. C. Lubensky, and E. J. Mele, Phys. Rev. B **40**, 2631 (1989).

<sup>10</sup> M. Andersson and S. Östlund, (unpublished).

<sup>11</sup> B. I. Shraiman and E. D. Siggia, Phys. Rev. B **46**, 8305 (1992); *ibid* Phys. Rev. Lett. **61**, 467 (1991).

<sup>12</sup> A. B. Eriksson, T. Einarsson, and S. Östlund, Phys. Rev. B **52**, 3662 (1995).

<sup>13</sup> Y. Hasegawa, P. Lederer, T. M. Rice, and P. B. Wiegmann, Phys. Rev. Lett. **63**, 907 (1989).